LARGE SCALE VOLUMETRIC FLOW MEASUREMENTS IN A TURBULENT BOUNDARY LAYER

D. Schanz[1,c], R. Geisler[1], C. Voss[1], M. Novara[1], T. Jahn[1], U. Dierksheide[2], A. Schröder[1]

[1]German Aerospace Center (DLR), Institute of Aerodynamics and Flow Technology,
Department of Experimental Methods, Göttingen, 37073, Germany
[2]LaVision GmbH, Göttingen, 37081, Germany
[c]Corresponding author: Tel.: +495517092883; Email: daniel.schanz@dlr.de

KEYWORDS:
Main subjects: turbulent boundary layer, superstructures, flow visualization
Fluid: low-speed air flow
Visualization method(s): Lagrangian Particle Tracking, data assimilation
Other keywords: Shake-The-Box, FlowFit

ABSTRACT: *The aim of this work is to capture the spatiotemporal dynamics of large-scale flow structures in a turbulent boundary layer flow in a volumetric and time-resolved way. The applied means are dense Lagrangian Particle Tracking of Helium-Filled Soap Bubbles (HFSBs) using the Shake-The-Box (STB) algorithm and a subsequent interpolation to a regular grid using the physically regularized FlowFit method. The presented experiment was performed as a pre-test to a full campaign to be held in August 2018 at the Atmospheric wind tunnel at the University of the armed forces in Munich, Germany. This test demonstrates the principle applicability of the measurement techniques to a low-speed wind tunnel environment and shows that high spatial accuracy and resolution can be reached despite of a large measurement volume. Problems were encountered achieving a homogeneous bubble distribution and in deploying large amounts of bubbles, while not disturbing the flow.*

1 Introduction

The understanding of the formation and the dynamics of very-large scale coherent structures within turbulent boundary layers (TBL) and their influence on the wall shear stress is an important research topic in aerodynamic flows at high Reynolds numbers not attainable by DNS. [1] showed that eddies with streamwise lengths of 10–20 δ are present in the logarithmic region of wall-bounded flows by compiling results from existing measurements and numerical simulations. [2] found streamwise energetic modes with wavelengths up to 14 pipe radii within fully developed turbulent pipe flow. They accounted the alignment of packets of hairpin-vortices as responsible for the creation of such structures and termed them ‘very large scale motion’ (VLSM). Indications of the existence of similar flow structures within the log-region of TBLs were given by [3], as well as [4]. They were able to document the existence of long stripes of negative or positive streamwise velocity fluctuations (u') within these domains. Both publications relied on measurements using the method of particle imaging velocimetry (PIV) with a streamwise length of the investigation area around two times the boundary layer thickness (δ). Therefore the full extent of the found structures could not be examined. [5] and again [6] confirmed these results using a similar PIV-setup. Additionally, they performed measurements using a hotwire rake, covering a spanwise distance of more than one δ with eleven hot-wire probes. By applying Taylor’s hypothesis on the obtained time-series, they were able to extract quasi-instantaneous snapshots of the flow structures at several heights above the wall. In many of these snapshots, very long structures of positive and negative u’ can be seen, frequently exceeding a length of 20 δ. These regions of negative and positive u’ typically appear besides each other and show a meandering

behavior in spanwise direction. The authors account this meandering to the fact that the length scales indicated by single-point statistics were much shorter (around 6 δ). Due to the large extent of the found features, the authors termed them 'superstructures'. As shown by experimental data [7][8], these superstructures seem to directly interact with small-scale structures near the wall (leaving a 'footprint'). This impact on the conditions near the wall is of particular interest for the wall-shear stress induced drag production, as the large-scale structures underlie outer scaling (their extent is dependent on δ and therefore also dependent on the Reynolds number), while it was assumed that near-wall structures do not. A further examination of the formation and evolution of superstructures in their fully temporal and spatial extension is therefore of major interest for a better understanding of turbulent (wall bounded) flows in general.

The aim of this work is to capture the large-scale development of a turbulent boundary layer in a both volumetric and time-resolved way. The applied means to achieve this goal are dense Lagrangian Particle Tracking of Helium-Filled Soap Bubbles (HFSBs) using the *Shake-The-Box* (STB) algorithm [9] and a subsequent interpolation to a regular grid using the physically regularized *FlowFit* method [10]. The presented experiment was performed as a pre-test to a full campaign to be held in August 2018 at the atmospheric wind tunnel (AWM) at the University of the armed forces in Munich, Germany.

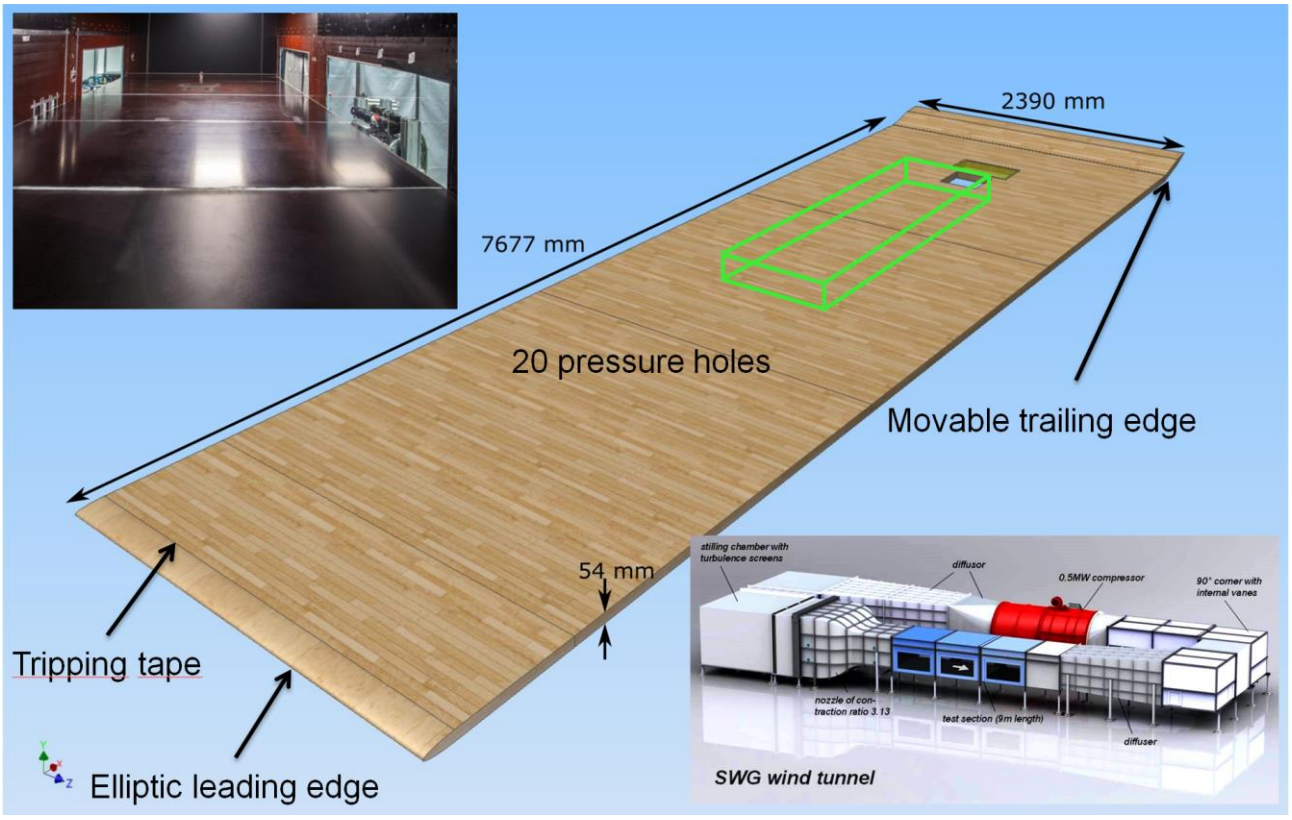

Fig. 1. 3D sketch of the splitting plate, as installed in the Seitenwindkanal Göttingen (SWG) (see right insert). The left insert shows a photograph of the plate in the tunnel. The measurement volume is indicated by the green box.

2 Experimental Methods and Setup

It has been shown recently that tracking HFSBs in flows up to approx. 20 m/s is possible at high accuracies and bubble numbers due to the large amounts of light reflected by the bubble surface and the resulting very good image quality [11][12][13].
Illuminating the bubbles with state-of-the-art high power pulsed LED arrays allows for scaling the instantaneous measurement volume up to the cubic meter range. The tracing fidelity of such bubbles has been shown to be sufficient for low-speed wind tunnel experiments [14].
Here, the measurement principle was applied to a TBL flow, which was created in the Seitenwindkanal at DLR Göttingen (SWG). To this end, a splitting plate of 7.67 meter length and 2.39 m width was installed in the 9 m long test section of the tunnel (see Fig. 1). A tripping tape was applied right after the elliptical leading edge. Close to the end of the splitting plate, a system of four newly developed high-power LED arrays [15] was installed on one side of the tunnel, illuminating the plate spanwise and tangentially over a streamwise length of 1.5 m and a height of approx. 0.25 m (see Fig. 1 and Fig. 2). Mirrors were installed on the opposite wind tunnel side wall, back-reflecting the volumetric light sheet, in order to increase the effective light output. Due to the low opening angle of the LEDs (6°), the light volume remains well confined within the measurement volume.

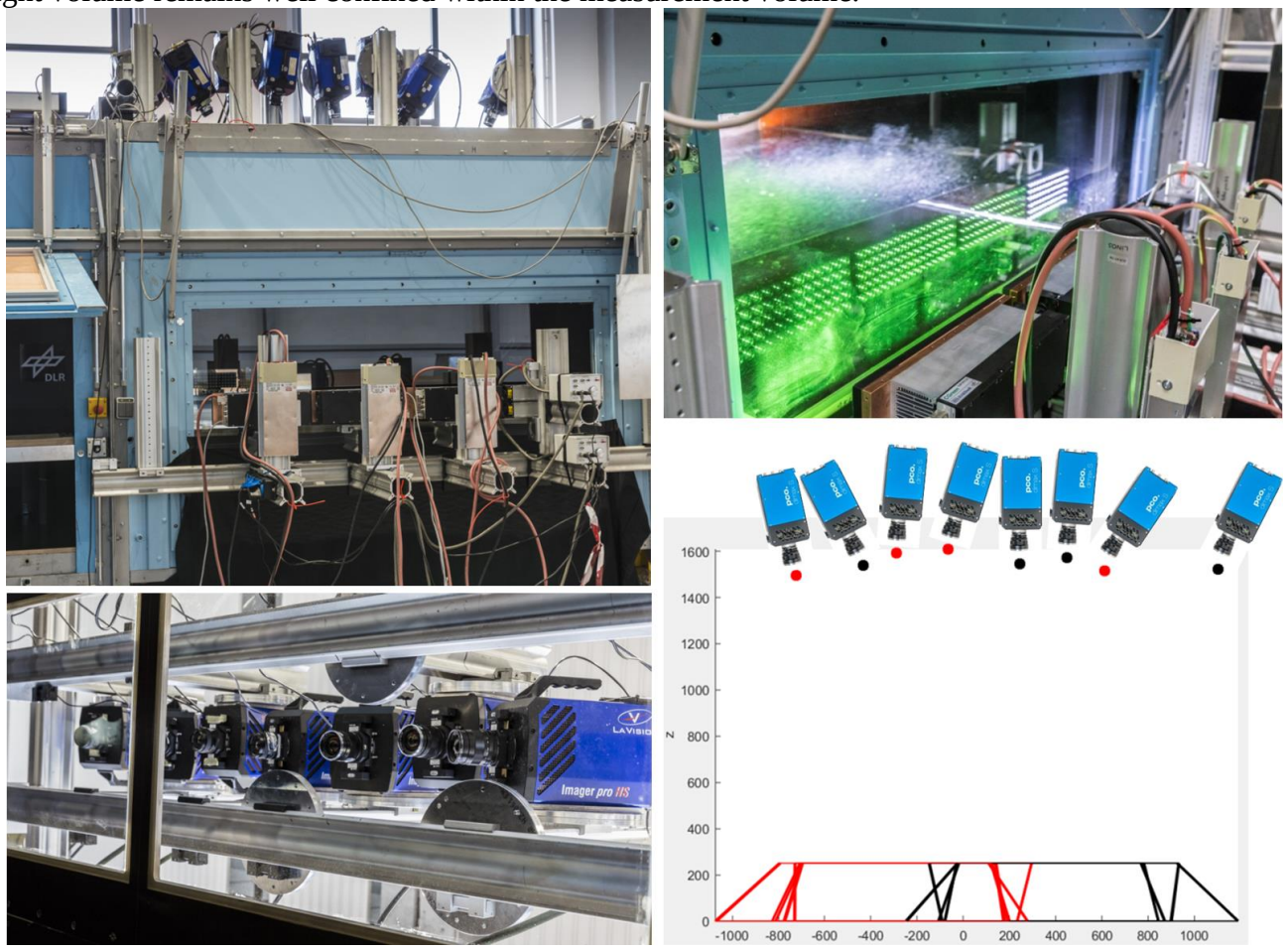

Fig. 2. (Left, up) Overview of the LED arrays and cameras installed at SWG; (Right, up) Four LED arrays, installed at the wind tunnel side, illuminating the HFSB inside theTBL flow through a glass window; (Left, down) the camera system viewed through the windows in the ceiling of the tunnel. (Right, down) Sketch of the fields of view of two overlapping four-camera systems, forming one large connected measurement field of 1.5 m length.

The illuminated volume was imaged by two systems of four high-speed cameras (LaVision Imager Pro HS) each, which were installed on top of the wind tunnel test section, viewing through the illuminated region onto the darkened flat plate. Each four-camera system was imaging a common volume of approx. 90 × 60 × 25 cm^3 (streamwise × spanwise × wall-normal). The two volumes overlapped for around 30 cm in streamwise direction, yielding a total volume of 150 × 60 × 25 cm^3 (225 liters, see Fig. 2). The cameras were equipped with 35 mm Carl Zeiss Distagon lenses, which were tilted according to the Scheimpflug condition.
The calibration of the camera viewing angles was performed using a 2.3 m × 1.0 m dot pattern calibration target, which was translated by 95 mm in wall-normal direction. Using a custom approach of the Volume-Self-Calibration [16], a common calibration for all eight cameras was created, so that bubbles could be seamlessly tracked when crossing from one system to the other, without the need of stitching. The optical transfer function (OTF) of the particles was calibrated according to [17].
An array of 100 HFSB nozzles was installed at the end of the settling chamber, each outputting ~35.000 bubbles of 300 µm diameter per second. The array consisted of five wing-profile blades, each with insets for 20 nozzles (see Fig. 3). The flow rates of soap, air and helium were tuned using a LaVision HFSB controller. The height of the array was chosen such that a minor part of the generated bubbles was sheared off by the leading edge of the splitting plate, thus ensuring adequate seeding of the near-wall region.

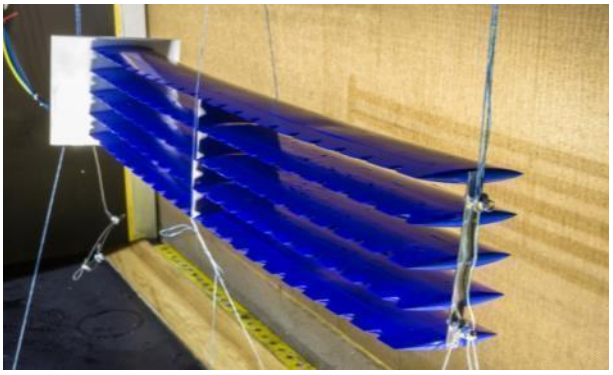

Fig. 3: Five wing-shaped blades, each housing 20 HFSB nozzles, as installed in the settling chamber of SWG.

The recordings were carried out at free stream velocities of $U_{Inf} = 5.7$ m/s, $U_{Inf} = 13.7$ m/s and $U_{Inf} = 22.7$ m/s at repetition rates of 1 and 2 kHz. Depending on U_{Inf}, the LED pulse duration t_P was adjusted, in order to minimize temporal blurring of the particle images at higher flow velocities. Values between $t_P = 99$ µs and $t_P = 30$ µs were used. With reduction of t_P, the illumination is lowered, however all cases yielded sufficiently bright peaks for STB particle tracking . Fig. 4 shows exemplary images at $t_P = 49.5$ µs ($U_{Inf} = 13.7$ m/s). The images were preprocessed by subtracting the sliding minimum over a kernel of 20 images.

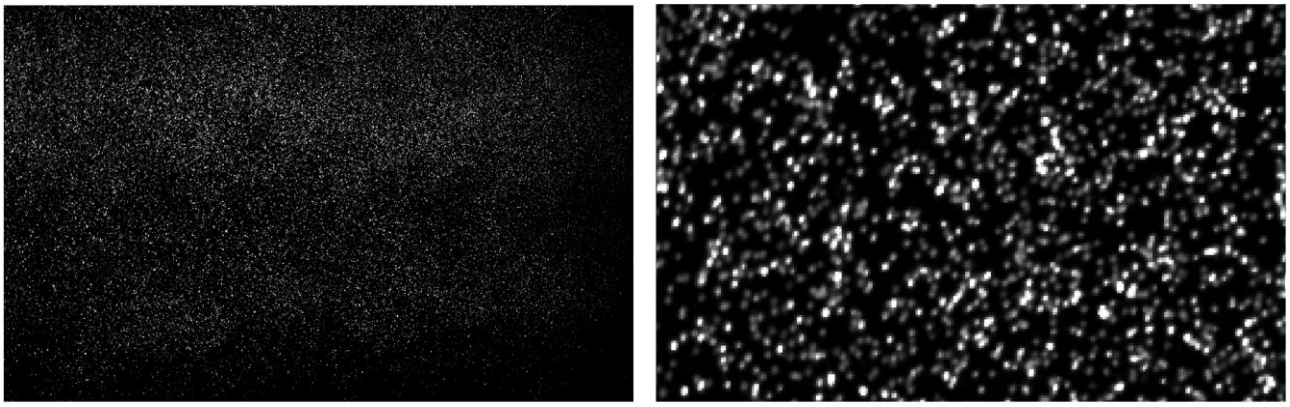

Fig. 4. Exemplary camera images (Left: full view, right:detail view), showcasing the particle image quality

From the camera images, Lagrangian particle tracks were reconstructed using the Shake-The-Box method [9]. An updated and extended version of the DLR in-house code was used [18]. The parameters of the internally applied method of Iterative Particle Reconstruction (IPR) [19] were as follows: the allowed triangulation error was set to 0.9 pixel, the height threshold for the 2D peak search was 25 counts, the number of particle location updates ('shake iterations) was 6 and the number of IPR iterations (triangulation on residual images + shaking) was 4. The following parameters were applied for the STB tracking part: The search radius for new tracks in the initialization phase was 9 pixels, with a pre-shift in streamwise direction of 8 pixels. For separation of real tracks from false track candidates, the maximum deviation from a Wiener-filter fit on four positions was set to 1.2 pixels per particle. With these setting, a large fraction of the present particle tracks (between 60 and 75 %, depending on the seeding density) were identified after the first four time-steps. From there on, the location of the particles of the known tracks for the next time step was predicted using a Wiener filter. The predicted particle positions were treated by eight iterations of shaking to correct prediction errors. New particles were triangulated from the residual images. The search for new tracks was aided by a predictor, which was constructed from a Gaussian average of the velocities of four neighboring particles with a search radius of 7 pixels. Additional particle tracks are identified and the algorithm converges within 20 to 30 time-steps.
After particle tracking was performed using STB, found particle positions are filtered with a continuous function consisting of cubic B-splines ("TrackFit") [10]. The found discrete point information was interpolated to an Eulerian grid using the FlowFit algorithm [10], which applies physical constraints (data assimilation methods) to increase the spatial resolution beyond the sampling by the particles. These results can be used for examination of instantaneous flow structures.

3 Results

Three different free stream velocities were examined: $U_{Inf} = 5.7$ m/s (Re_θ = 4150 at the most upstream position of the measurement volume, Re_θ = 4900 at the most downstream position), $U_{Inf} = 13.7$ m/s (Re_θ = 10,400 - 12,200) and $U_{Inf} = 22.7$ m/s (Re_θ = 15,000 - 17,600).
Due to the fixed production rate of the HFSB nozzle arrays, the particle image density on the camera images is proportional to U_{Inf}. At the lowest velocity, local values of the particle image density up to 0.08 particles per pixel are reached, however the particle distribution was quite uneven (as can be seen in Fig. 4). For this case, around 166.000 bubbles could be tracked within every time-step for time-series

of 4.800 images (after convergence of the STB algorithm). Judging from residual images, nearly all imaged bubbles were identified. Fig. 5 (Left) shows different views of a single time-step from such an evaluation. It can be seen that the outer regions of the boundary layer are subject to changes in particle density due to the entrainment of un-seeded air and some uneven production of the nozzles. However, the more interesting lower parts of the boundary layer, that experience turbulent mixing, are homogenously seeded. The very near-wall region could mostly not be captured due to the large size of the tracer particles in relation to the strong shear close to the wall (see side view in Fig. 5). When looking at a wall-parallel slice in the logarithmic part of the boundary layer (between z=30 mm and z=60mm) large, elongated structures of positive and negative u' can be identified, showcasing the typical meandering behavior of superstructures. In single snapshots, the length of these structures frequently exceeds 10 boundary layer thicknesses (δ_{99}).

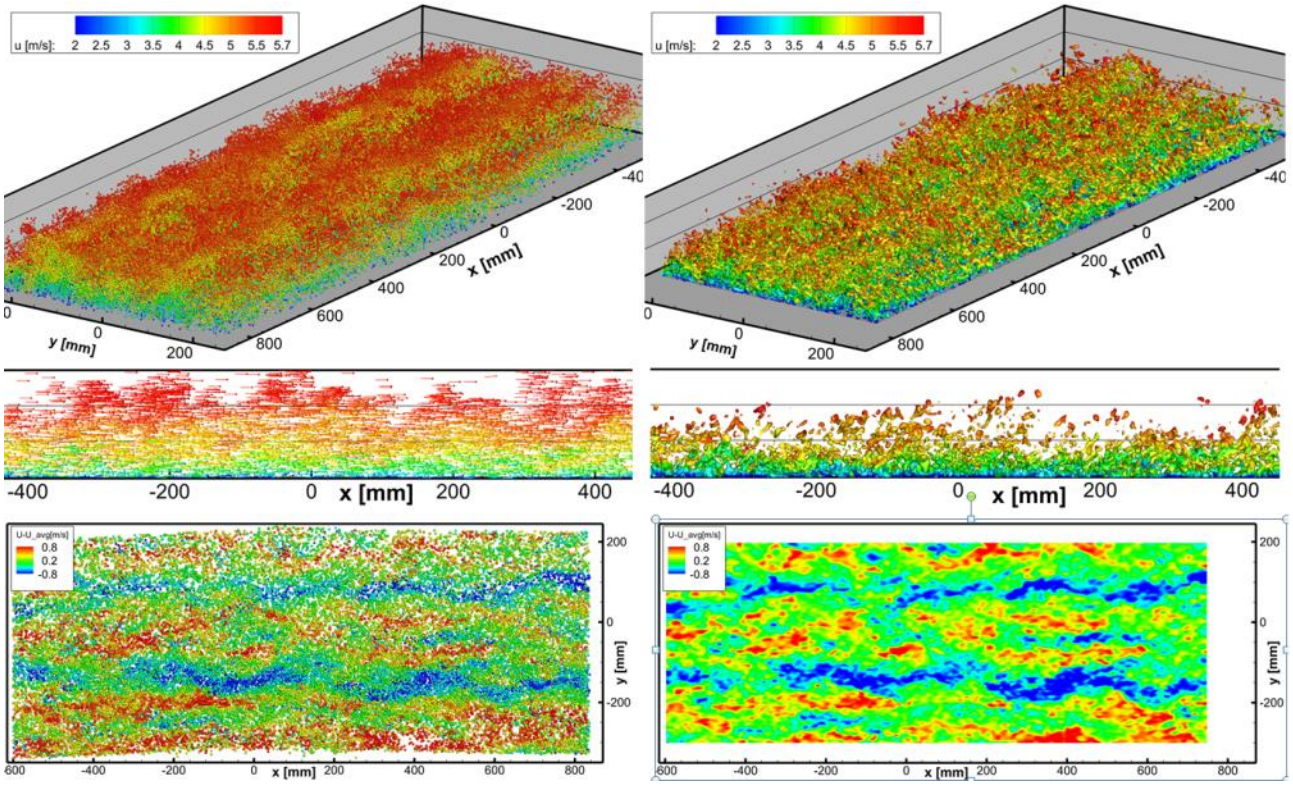

Fig. 5. Instantaneous results at U_{inf}=5.7 m/s. (Left column): All tracked particles (~ 166.000) at single time-step; flow – parallel plane 5 cm thickness, showing particle tracks; Superstructures in a wall-parallel slice (30 – 60 mm above the wall), cc. by streamwise velocity fluctuations (Right column): FlowFit results of the same time-step. Iso-surfaces of Q-criterion (Q = 6.500 1/s^2), and a wall parallel slice, cc. by streamwise velocity fluctuations.

Regularized interpolation of the particle data onto a regular grid using FlowFit allows examination of the flow structures. The exemplary result given in Fig. 5 reveals a multitude of resolved flow structures, despite the large measurement volume. Vortices of different size and strength are visualized by the Q-criterion; the smallest resolvable structures (showing temporal coherence when examining a time-series) are only few mm in diameter. Compared to a mean bubble distance of d = 6.37 mm this demonstrates the ability of the Navier-Stokes regularizid data assimilation scheme FlowFit to increase the spatial resolution beyond sampling. Looking at a streamwise slice, an inclination of the structures in flow direction is evident, which has been reported as well for large hairpin-like structures in the

literature (Adrian 2007). As expected, the occurrence of major structures is limited by the boundary layer thickness (here $\delta_{99} \approx 112$ mm). A wall-parallel slice through the volume at z =42 mm reveals the same largescale structures as already visible in the particle representation.

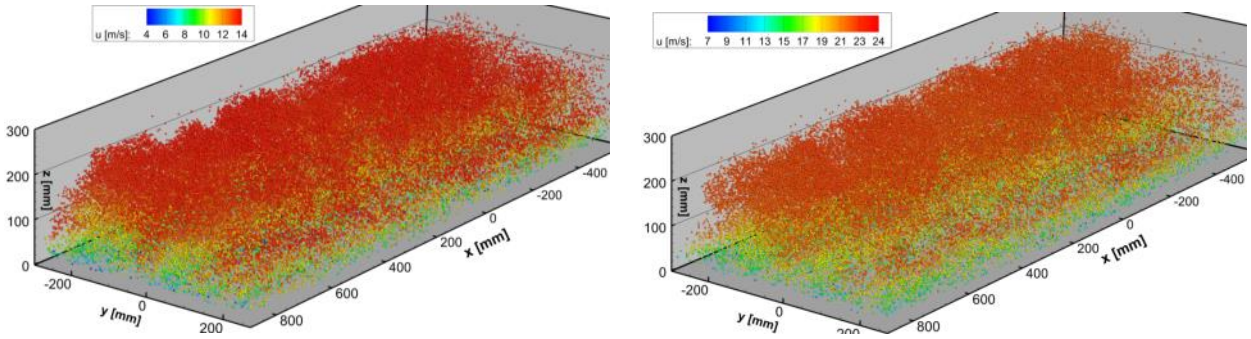

Fig. 6. Particle field at single time-step at U_{inf} = 13.7 m/s (Left) and U_{inf} = 22.7 m/s (Right). Color-coding by streamwise velocity

For the higher flow velocities the tracking was equally successful, despite the reduced illumination time. 90.000 bubbles could be tracked per time-step at $U_{Inf} = 13.7$ m/s and 74.000 at $U_{Inf} = 22.7$ m/s. These numbers reflect the reduction in particle image density due to the increase in mass flow and velocity. Fig. 6 shows exemplary particle field for both velocities. Tracer bubbles can be found up to around 250 mm above the wall, however the particle distribution gets more and more inhomogeneous with increased velocities (see also Fig. 7, Left).

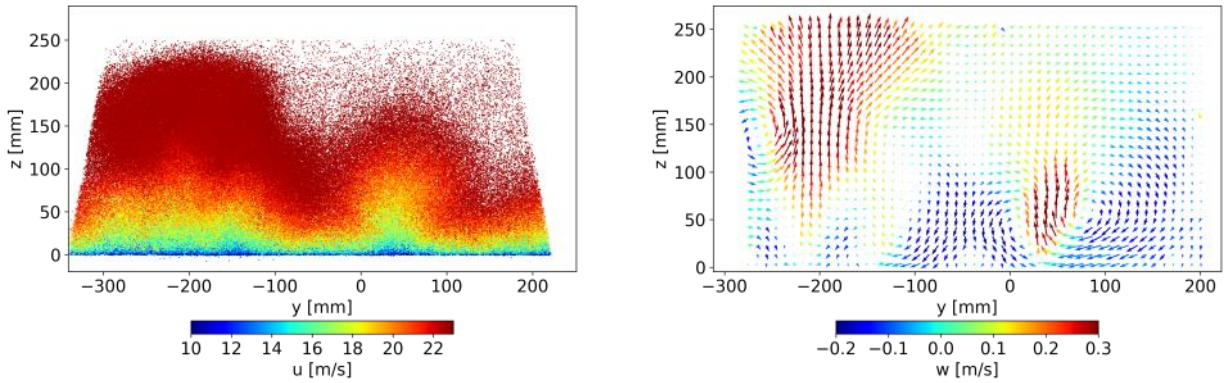

Fig. 7. (Left) Particles (sum of several time-steps) within streamwise slice of 120 mm thickness at U_{inf} = 22.7 m/s; (Right) Bin-averaged velocity field (over 4800 images) in streamwise direction at U_{inf}=22.7 m/s, showing persistent vortices in streamwise direction, caused by the interaction of the HFSB rakes with the flow.

Persistent longitudinal 'hills' and 'valleys' of particles can be recognized. This distribution is a first sign of disturbances caused by the HFSB nozzle rakes. Due to the fine meshes used in SWG, the bubbles had to be produced close to the measurement area. The arrays were positioned approx. 3 m in front of the splitting plate, in a region of contraction. Due to the bent streamlines, an optimal positioning of the nozzle wings without any angle of attack was not possible. Therefore, flow disturbances were induced, especially on the edges (tips) of the nozzle wings. Persistent vortices in stream-wise direction were created, leading to a permanent entrainment of clean air from the sides

(visible as valleys in the bubble distribution). Beside these regions, the well-seeded fluid close to the wall is pressed upwards (visible as hills).

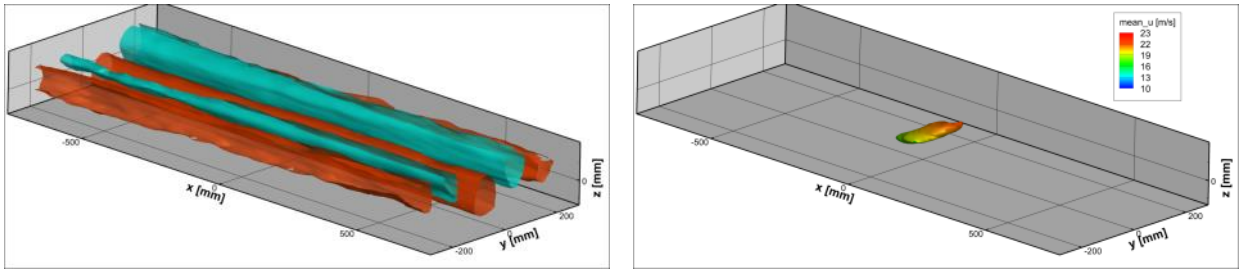

Fig. 8. 3D Two-point correlation iso-surfaces of streamwise (u-u, Left) and wall-normal component (w-w, Right) at U_{inf}=22.7 m/s

These persistent flow structures can be quantified by averaging the particle tracking results of a full run (4,800 images) in three-dimensional bins. Fig. 7 (Right) shows a span-wise plane of such an average flow field at U_{inf} = 22.7 m/s, with bins of size 120 × 20 × 20 mm^3. A footprint of the induced system of vortices can be seen, with maximum average wall-normal velocities of 0.4 m/s. When performing three-dimensional two-point correlations for U_{inf} = 22.7 m/s, these structures are clearly visible as long isosurface-tubes in the streamwise component (u-u, see Fig. 8). The wall-normal component (w-w) shows a shape that is expected given the inclined vortex structures within a turbulent boundary layer.
As a result of these circumstances, the logarithmic layer is dominated by long, persistent streaks of positive and negative velocity fluctuation, spanning the whole measurement domain (see Fig. 9). It is evident that in the current investigation, at least for higher velocities, the creation and life of superstructures is influenced too much by the external disturbances for any meaningful examination.

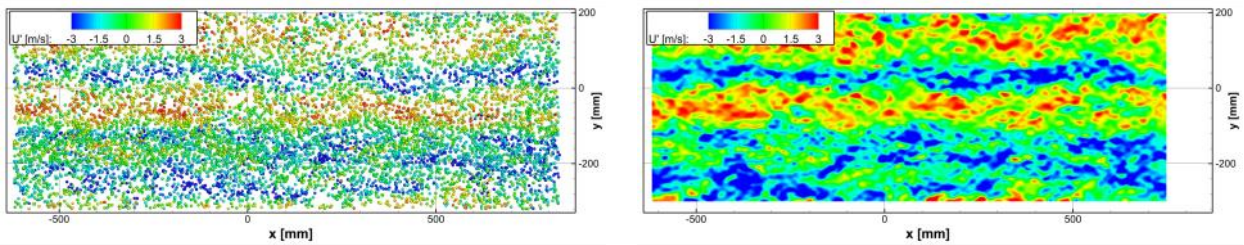

Fig. 9. (Left) Wall-parallel slice (z =30-60 mm) through tracked particles of single time-step at U_{inf}=22.7 m/s, color-coded by streamwise fluctuations (u'). Persistent, elongated regions of delayed and accelerated flow can be seen. (Right) Wall –parallel slice (z = 45 mm) of FlowFit result of the same time-step

On the other hand, the presented work was merely a trial for the actual experimental campaign to be carried out at the atmospheric wind tunnel (AWM) in Munich in August 2018. The aim was to identify possible challenges and to verify that the measurement technology is applicable in a wind-tunnel environment. The latter can clearly be seen as a success, as the flow could be successfully captured under all experimental circumstances. To further support this statement, Fig. 10 shows a full-field result of the FlowFit evaluation at U_{inf}=13.7 m/s and U_{inf}=22.7 m/s. Despite a lower number of available tracer particles and the higher Reynolds-number of the flows, the main vortical structures are still resolved. Temporal coherence of the structures is still present, albeit less pronounced than for the case at U_{inf}=5.7 m/s.

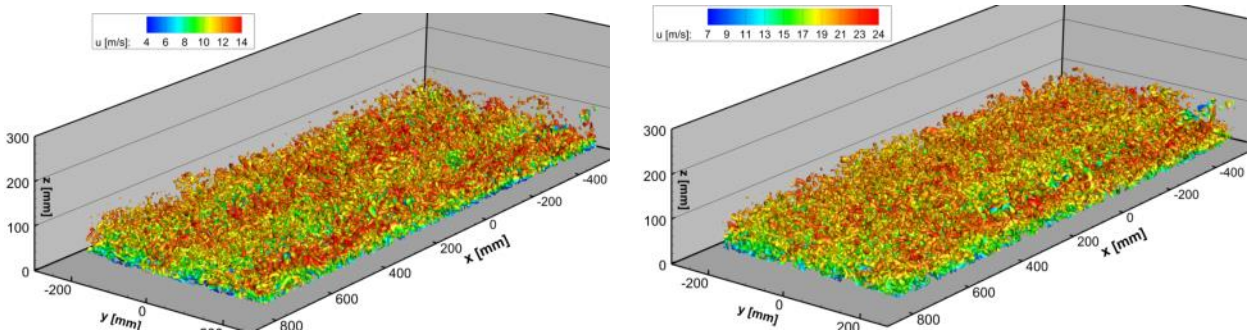

Fig. 10. Flow structures, visualized by Q-criterion of FlowFit evaluation result of single time-step at U_{inf}=13.7 m/s (Left, Q = 20,000) and U_{inf}=22.7 m/s (Right, Q = 36,500). Color-coding by streamwise velocity

Conclusions

An experiment was conducted at the Seitenwindkanal at DLR Göttingen (SWG), investigating a turbulent boundary layer flow spatially and temporally in a large volume of approx. 225 liters. It has been shown that large-scale, time resolved volumetric flow measurements can be realized at high spatial resolution in a wind tunnel environment at relevant flow velocities (currently up to around 25 m/s, further increases are foreseeable). The key ingredients for such experiments are the use of Helium-filled soap bubbles as tracers, being illuminated by high-power LED arrays. The resulting images are well-suited for Lagrangian Particle Tracking using Shake-The-Box; the regularized interpolation using the FlowFit algorithm allows to further increase the spatial resolution.
The seeding system was identified as a possible source of flow disturbances. In order to produce bubbles in such high numbers to sufficiently seed the flow, many nozzles have to be installed within the tunnel. Depending on the size and the shape of the nozzle arrays, it can be not easy to position them in a way, which does not influence the flow and the properties one might be interested in. For the current investigation, the arrays were not optimized and had to be put very close to the measurement domain. As a result, the flow was clearly biased by persistent longitudinal vortices. One measure to limit disturbances would be to extend the nozzle profiles to the wind tunnel wall, thus avoiding any wing tip vortices. Positioning the arrays further upstream, possibly in regions with low flow velocities, would give more time for distribution and dissipation of such disturbances. These learned lessons will be applied in the main wind tunnel experiment, to be carried out in August 2018, which will concentrate on the identification of turbulent superstructures and the characterization of their spatial and temporal development.

Acknowledgements

The authors would like to thank Janos Agocs, Carsten Fuchs, Tobias Kleindienst, Hartmut Mattner, Dirk Otter, Kamil Ludwikowski and Dirk Michaelis for their help during the setup and execution of the experiment. The realization of the camera system was only possible through the help of the Technical University of Delft and the University of the armed forces in Munich, each supplying four cameras.
The work has been conducted in the scope of the DFG-project “Lagrangian and Eulerian analysis of superstructures in turbulent flows based on large-scale, time-resolved and volumetric measurements using Shake-The-Box and PIV”, as part of the DFG priority programme 1881 “Turbulent Superstructures”.

References

[1] Jimenez J (1998), The Largest Scales of Turbulent Wall Flows, CTR Annual Research Briefs: 137-54, University, Stanford

[2] Kim KC, Adrian RJ (1999), Very large-scale motion in the outer layer. Phys. Fluids 11: 417-422

[3] Tomkins CD, Adrian R.J (2003), Spanwise structure and scale growth in turbulent boundary layers. J. Fluid Mech. 490:37-74

[4] Ganapathisubramani, B., Longmire, E.K., Marusic, I. (2003), Characteristics of vortex packets in turbulent boundary layers. J. Fluid Mech. 478: 35–46

[5] Hutchins N, Marusic I (2007), Evidence of very long meandering features in the logarithmic region of turbulent boundary layers. J. Fluid Mech. 579:1-28

[6] Marusic I, McKeon BJ, Monkewitz PA, Nagib HM, Smits AJ, Sreenivasan KR (2010), Wall-bounded turbulent flows at high Reynolds numbers: recent advances and key issues, Phys. Fluids 22, 065103

[7] Hutchins N, Monty JP, Ganapathisubramani B, Ng HCH, Marusic I (2011), Three-dimensional structure of a high-Reynolds-number turbulent boundary layer, J. Fluid Mech. 673: 255-285, DOI: 10.1017/ S0022112010006245

[8] de Silva CM, Gnanamanickam EP, Atkinson C, Buchmann NA, Hutchins N, Soria J, Marusic I (2014), High spatial range velocity measurements in a high Reynolds number turbulent boundary layer, Physics of Fluids, 26, 025117, DOI:10.1063/1.4866458

[9] Schanz D, Gesemann S, Schroder A (2016) Shake-The-Box: Lagrangian particle tracking at high particle image densities. Exp Fluids, 57(5)

[10] Gesemann S, Huhn F, Schanz D, Schroder A (2016): From noisy particle tracks to velocity, acceleration and pressure fields using B-splines and penalties. 18th Int. Symp. on Appl. of Laser and Imaging Tech. to Fluid Mech. Lisbon, Portugal, July 4 – 7 2016

[11] Schanz D, Huhn F, Gesemann S, Dierksheide U, van de Meerendonk R, Manovski P, Schröder A (2016) Towards high-resolution 30 flow field measurements at the cubic meter scale. 18th Int. Symp. on Appl. of Laser and Imaging Tech. to Fluid Mech. Lisbon, Portugal, July 4 – 7 2016

[12] Huhn F, Schanz D, Gesemann S, Dierksheide U, van de Meerendonk R, Schroder A (2017) Large-scale volumetric flow measurement in a pure thermal plume by dense tracking of helium-lied soap bubbles, Exp. Fluids 58:116.

[13] Huhn, F., Schanz, D., Manovski, P. et al. (2018) Exp Fluids 59: 81. https://doi.org/10.1007/s00348-018-2533-0

[14] Scarano F, Ghaemi S, Caridi GAC, Bosbach J, Dierksheide U, Sciacchitano A (2015) On the use of helium-filled soap bubbles for large-scale tomographic PIV in wind tunnel experiments; Exp. Fluids 56:42

[15] Stasicki B, Schroder A, Boden F, Ludwikowski K (2017) High-power LED light sources for optical measurement systems operated in continuous and overdriven pulsed modes, Optical Measurement Systems for Industrial Inspection X 10329, 103292J

[16] Wieneke B (2008) Volume self-calibration for 3D particle image velocimetry. Exp Fluids, 45:549-556

[17] Schanz D, Gesemann S, Schröder A, Wieneke B, Novara M (2013) Non-uniform optical transfer functions in particle imaging: calibration and application to tomographic reconstruction. Meas Sci Technol 24 024009

[18] Jahn T (2017) Volumetrische Strömungsvermessung: Eine Implementierung von Shake-The-Box. Masterarbeit, Georg-August-Universität Göttingen & DLR Göttingen.

[19] Wieneke B (2013) Iterative reconstruction of volumetric particle distribution. Meas. Sci. Technol. 24:024008